



HAL
open science

North Atlantic ice-rafting, ocean and atmospheric circulation during the Holocene: insights from Western Mediterranean speleothems

Yassine Ait Brahim, J. Wassenburg, L. Sha, F. Cruz, M. Deininger, Abdel Sifeddine, Lhoussaine Bouchaou, Christoph Spötl, R. Edwards, H. Cheng

► **To cite this version:**

Yassine Ait Brahim, J. Wassenburg, L. Sha, F. Cruz, M. Deininger, et al.. North Atlantic ice-rafting, ocean and atmospheric circulation during the Holocene: insights from Western Mediterranean speleothems. *Geophysical Research Letters*, 2019, 46 (13), pp.7614-7623. 10.1029/2019GL082405 . hal-02416060

HAL Id: hal-02416060

<https://hal.science/hal-02416060v1>

Submitted on 21 Sep 2021

HAL is a multi-disciplinary open access archive for the deposit and dissemination of scientific research documents, whether they are published or not. The documents may come from teaching and research institutions in France or abroad, or from public or private research centers.

L'archive ouverte pluridisciplinaire **HAL**, est destinée au dépôt et à la diffusion de documents scientifiques de niveau recherche, publiés ou non, émanant des établissements d'enseignement et de recherche français ou étrangers, des laboratoires publics ou privés.

Geophysical Research Letters

RESEARCH LETTER

10.1029/2019GL082405

Key Points:

- A high-resolution multi-speleothem rainfall index describes the Holocene rainfall variability in the Western Mediterranean
- On centennial to millennial scales, negative NAO-like conditions were likely associated with the Early and Late Holocene ice-rafting events
- Different mechanisms involving north and south shifts of the westerly winds belt might contribute to ice-rafting and the AMOC slowdown

Supporting Information:

- Supporting Information S1

Correspondence to:

Y. Ait Brahim,
aitbrahim@xjtu.edu.cn

Citation:

Ait Brahim, Y., Wassenburg, J. A., Sha, L., Cruz, F. W., Deininger, M., Sifeddine, A., et al (2019). North Atlantic ice-rafting, ocean and atmospheric circulation during the Holocene: Insights from Western Mediterranean speleothems. *Geophysical Research Letters*, 46, 7614–7623. <https://doi.org/10.1029/2019GL082405>






Received 11 FEB 2019

Accepted 10 JUN 2019

Accepted article online 17 JUN 2019

Published online 3 JUL 2019

North Atlantic Ice-Rafting, Ocean and Atmospheric Circulation During the Holocene: Insights From Western Mediterranean Speleothems

Y. Ait Brahim¹ , J. A. Wassenburg², L. Sha¹, F. W. Cruz³ , M. Deininger⁴, A. Sifeddine⁵, L. Bouchaou⁶ , Christoph Spötl⁷ , R. L. Edwards⁸, and H. Cheng^{1,8} 

¹Institute of Global Environmental Change, Xi'an Jiaotong University, Xi'an, China, ²Climate Geochemistry Department, Max Planck Institute for Chemistry, Mainz, Germany, ³Instituto de Geociências, Universidade de São Paulo, São Paulo, Brazil, ⁴Institute of Geoscience, Johannes Gutenberg University Mainz, Mainz, Germany, ⁵IRD-Sorbonne Universités (UPMC, CNRS, MNHN) UMR LOCEAN, Centre IRD, Bondy, France, ⁶Laboratory of Applied Geology and Geo-Environment, Ibn Zohr University, Agadir, Morocco, ⁷Institute of Geology, University of Innsbruck, Innsbruck, Austria, ⁸Department of Earth Sciences, University of Minnesota, Twin Cities, Minneapolis, MN, USA

Abstract In this study, we present a Holocene rainfall index based on three high-resolution speleothem records from the Western Mediterranean, a region under the influence of the westerly winds belt modulated by the North Atlantic Oscillation (NAO). On centennial to millennial timescales, we show that the North Atlantic ice-rafting events were likely associated with negative NAO-like conditions during the Early Holocene and the Late Holocene. However, our data reveal that this is not clearly the case for the mid-Holocene ice-rafting events, during which we also show evidence of positive NAO-like patterns from other paleo-oceanographic and paleo-atmospheric data. Hence, contradictory mechanisms involving prolonged periods of both north and south shifts of the westerly winds belt (resembling positive and negative NAO-like patterns) might at least partially trigger or amplify the ice-rafting events and the slowdown of the Atlantic Meridional Overturning Circulation.

Plain Language Summary During the Holocene, periods of enhanced ice-rafting, associated with cooling and sea ice expansion in the North Atlantic high latitudes, have been recognized over distant regions. While the causes of these events are still a matter of debate, changes in the atmospheric circulation have been proposed as a potential trigger or amplifier. Here, we use speleothems to establish a precisely dated record of rainfall variability in the Western Mediterranean, a highly sensitive region to the westerly winds belt modulated by the North Atlantic Oscillation. Our results reveal new insights about the dynamics of NAO-like patterns during the Holocene. On centennial to millennial timescales, prolonged periods of both north and south shifts of the westerly winds belt might trigger or amplify the slowdown of the Atlantic Meridional Overturning Circulation and the North Atlantic ice-rafting. However, not all ice-rafting events are associated with either positive or negative NAO-like conditions.

1. Introduction

The North Atlantic Oscillation (NAO), expressed by the differential position and strength of the Azores High (AH) and the Icelandic Low (IL), is the main atmospheric mode of variability in the North Atlantic region during winter (Baker et al., 2015; Hurrell, 1995; Olsen et al., 2012; Ortega et al., 2015; Trouet et al., 2009; Visbeck et al., 2001; Wanner et al., 2001). The NAO modulates the strength and the direction of the westerly winds belt and consequently affects the climate patterns in regions around the North Atlantic. While the positions of the AH and the IL evolved to patterns resembling the modern modes of the NAO (Wang et al., 2012), the present-day interannual to decadal variability is believed to be different during the Holocene due to different forcing mechanisms, the retreat of the Laurentide Ice Sheet and the reduction in meltwater discharge into the North Atlantic (Wassenburg et al., 2016) and changes in the insolation (McDermott et al., 2011; Walczak et al., 2015). However, our understanding of NAO-like variability on centennial to millennial timescales is limited by the sparse number of climate records from key NAO regions.

The Holocene is characterized by multiple episodes of centennial timescale ice-rafting events (Bond events) in the northern North Atlantic (Bond et al., 1997, 2001). These events were recognized in deep-sea sediments but rarely replicated in well-dated terrestrial records. Several studies suggest that atmospheric circulation

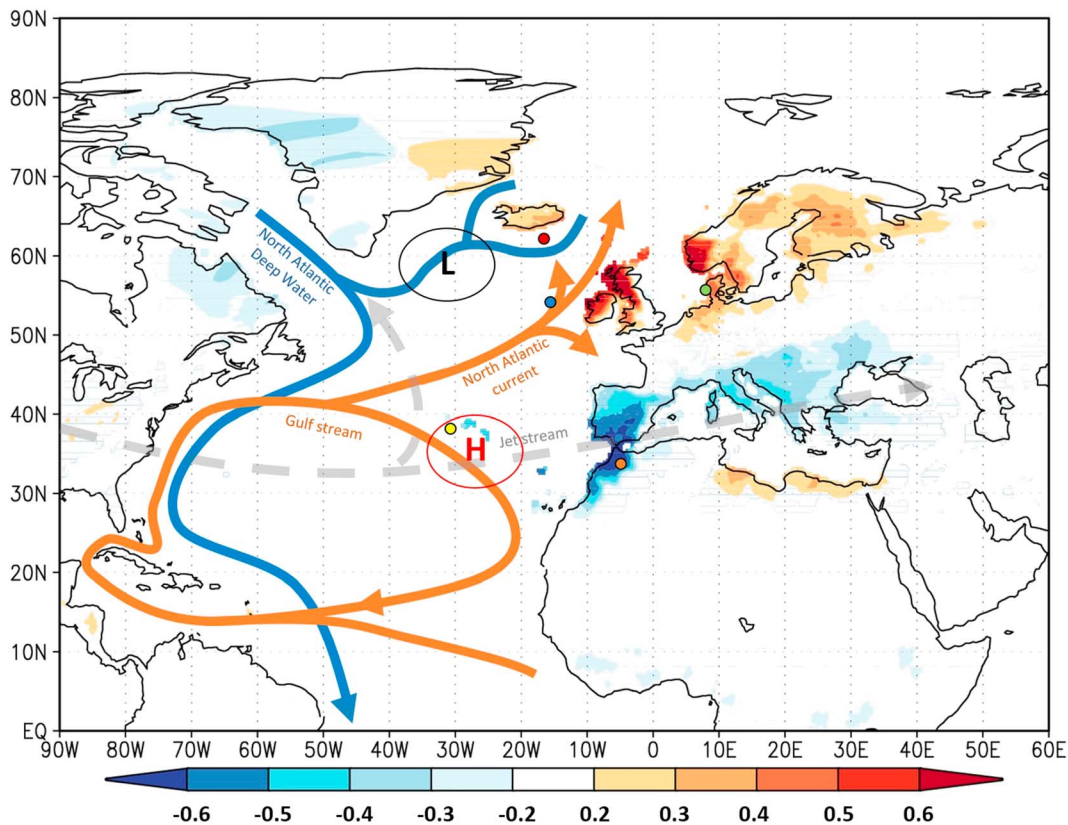


Figure 1. Correlation map between rainfall and the North Atlantic Oscillation (NAO) index during the winter season (December to March) over the period 1891–2016. The presented sea level pressure field and Jetstream location resembles negative NAO conditions associated with a southward shift of the westerly winds belt and storm track resulting in enhanced precipitation over the Western Mediterranean region. The correlation was calculated using the NAO-Gibraltar index (Jones et al., 1997) and the Global Precipitation Climatology Centre data set (Schneider et al., 2011). The main North Atlantic Ocean circulation currents and typical positions of the IL and the AH are shown as well. The red circle indicates the approximate location of the ocean core used for the reconstruction of the North Atlantic current activity (Thornalley et al., 2009). The blue circle indicates the approximate location of the ocean cores (MC52+V29-191) used for reconstructing the history of North Atlantic ice-rafting (Bond et al., 1997, 2001). The green circle indicates the approximate location of the sediment core used for the reconstruction of the storminess record (Goslin et al., 2018). The yellow circle indicates the approximate location sediment core used for the reconstruction of the position of the Azores Front (AF). (Repschläger et al., 2017). The orange circle indicates the location of Chaara and Grotte de Piste caves, where speleothems have been sampled for this study.

might have played a major role in triggering or amplifying these abrupt cooling episodes of the Holocene (e.g., Deininger et al., 2017; Goslin et al., 2018; Klus et al., 2018; Yang et al., 2016). However, the linkage between the atmospheric circulation and the ice-rafting events is still a matter of debate (e.g., Darby et al., 2012; Sorrel et al., 2012). Although Bond et al. (2001) indicate that North Atlantic land and sea surface temperature patterns are not in favor of a NAO-like forcing of the Bond events, modeling and other proxy data support that NAO-like conditions might have intervened in the enhancement of ice-rafting through a slowdown of the Atlantic Meridional Overturning Circulation (AMOC). However, contradictory mechanisms have been proposed, involving either northward or southward shifts of the westerly winds belt (akin to positive and negative NAO-like conditions; e.g., Yang et al., 2016; Deininger et al., 2017; Klus et al., 2018; Goslin et al., 2018). In this context, new high-resolution paleoclimate records from key NAO regions are crucial to improve our understanding of the North Atlantic hydroclimate variability, as well as to study the forcing mechanisms and the coupling between atmospheric and oceanic processes.

The Western Mediterranean is one of the most sensitive regions for the NAO due to its location at the north-eastern side of the AH (Figure 1). Negative (positive) NAO phases result in increased (decreased) winter precipitation (e.g., Knippertz et al., 2003; López-Moreno et al., 2011). On multidecadal to centennial timescales, the Atlantic Multidecadal Oscillation and solar irradiance have been shown to impact the Western Mediterranean climate through interactions with the NAO during the last millennium (Ait Brahim et al., 2018). Holocene climate reconstructions from the Western Mediterranean are available from lake, flood,

and marine archives (e.g., Benito et al., 2014; Fletcher et al., 2013; Morellón et al., 2018; Zielhofer et al., 2017, 2019). However, not all reconstructions represent the winter season only, which is the season when the NAO is most dominant. Robust information on past NAO variability and the involved mechanisms over the course of the entire Holocene is thus still lacking.

Here, we present two new precisely dated and high-resolution records of effective rainfall during the Holocene from Chaara cave in Northern Morocco, in addition to a previously published speleothem record from the same region (Wassenburg et al., 2016). A rainfall index is constructed from the three speleothem $\delta^{18}\text{O}$ records. Our results are interpreted in the light of paleo-oceanographic and atmospheric paleoclimate data in the North Atlantic. They provide new insights on the coupling between the North Atlantic atmospheric circulation associated with NAO-like patterns and the ice-raftering in the subpolar region.

2. Materials and Methods

2.1. Samples and Cave Site

We present two new high-resolution $\delta^{18}\text{O}$ records from two aragonite stalagmites (Cha1 and Cha2; Figure S1 in the supporting information). Both stalagmites were collected in 2010 below active drip sites, located 300 m behind the entrance of Chaara cave ($33^{\circ}57'21''\text{N}$, $4^{\circ}14'46''\text{W}$, 1260 m above sea level). Chaara cave developed within complex cave systems in the Liassic carbonate formations of the Middle Atlas region (Sabaoui et al., 2009; Taous et al., 2009; Wassenburg et al., 2012). The winter rainfall (December to March) accounts for 80% of the annual rainfall amount (about 1,000 mm/year), mainly related to Atlantic cyclones during the winter NAO (Ait Brahim et al., 2018; Wassenburg et al., 2016).

We compared our data to the GP2 speleothem $\delta^{18}\text{O}$ record from Grotte de Piste (Wassenburg et al., 2016), given that Grotte de Piste and Chaara Cave sites are only a few hundred meters apart (Ait Brahim et al., 2018).

2.2. Oxygen Isotope Analysis

$\delta^{18}\text{O}$ analyses were performed using a Thermo Finnigan Delta Plus Advantage at the Institute of Geoscience of the University of Sao Paulo (Brazil). Sampling was performed along the growth axis of each stalagmite using a micromill device. The $\delta^{18}\text{O}$ raw data were calculated using a calcite acid fractionation factor, and subsequently corrected to aragonite $\delta^{18}\text{O}$ values (Kim et al., 2007). The results are expressed in the Vienna Pee Dee belemnite standard. The analytical error is less than 0.15‰.

2.3. Age Model

Preliminary U/Th analyses were performed using a Neptune Multi-Collector Inductively Coupled Plasma Mass Spectrometers at the Isotope Laboratory of the University of Minnesota. Further U/Th analyses were carried out at the Institute of Global Environmental Change of Xi'an Jiaotong University. Uranium and thorium separation procedures are described by Edwards et al. (1987). The final age-depth model was constructed for each speleothem using the StalAge algorithm (Scholz & Hoffmann, 2011; Figure S2). Ages are reported in years BP, with 1950 CE as the year of reference.

2.4. Statistical Approach

A Monte Carlo (MC) approach was used to construct a composite from Cha1 and Cha2 $\delta^{18}\text{O}$ records by maximizing the correlation between both time series using the “intra-site correlation age modelling” (Fohlmeister, 2012). The model parameters were set using 10,000 MC simulations. Significance levels of the correlation and age uncertainties were determined using 100 runs of a first autoregressive process (AR1). Afterward, 1,000 MC runs were performed on each AR1. The same process was repeated between the Chaara cave (Cha1-Cha2) $\delta^{18}\text{O}$ composite and the GP2 $\delta^{18}\text{O}$ time series from Grotte de Piste to determine the MC records with the highest correlation between the two time series. These were used to perform a principal component analysis (PCA) to extract their common variability. The first axis of the PCA (PC1) was detrended using LOESS curve with a smoothing factor of 0.3. Significant periodicities in independent speleothem $\delta^{18}\text{O}$ records were defined by REDFIT analysis (Schulz & Mudelsee, 2002) using the PAST software (Hammer et al., 2001).

Given the large age uncertainties of the IRD record, expressed by the hematite-stained grains ocean cores MC52 and V29-191 (Bond et al., 2001), the quantification of the link between the speleothem-based Western Mediterranean rainfall index and the North Atlantic ice-rafted debris (IRD) is challenging. Therefore, to test if there is a significant ($p < 0.05$) correlation between our data and the IRD record, a MC approach was performed to shift the IRD record in time in accordance with its age uncertainties. For this, in each MC run, a new age model of the IRD record is calculated by varying the ages within the 2-sigma age uncertainty limits and using a linear interpolation between these new ages to construct a new proxy (IRD) age model/record. Then, having the higher temporal resolution, our data are interpolated to the time resolution of the new IRD record and a linear correlation is calculated between the new IRD record and the interpolated PC1. This procedure is repeated at least 2,000 times, resulting in at least 2,000 new IRD records with modified age models compared to original IRD record. Because of the large age uncertainties of the IRD record, both positive and negative correlations are observed (Figure S3). Therefore, we used the correlation results between PC1 and the tuned new IRD records to test that the proposed mechanisms, which we discuss below, are possible over different time periods (Figure S4).

3. Results and Discussion

3.1. Description of Speleothems $\delta^{18}\text{O}$ Records

The age model of Cha1 is based on 50 Th/U dates (Table S1) and 1,593 $\delta^{18}\text{O}$ data points, while the Cha2 record is constructed using 44 Th/U dates (Table S2) and 669 $\delta^{18}\text{O}$ data points. The growth rate of Cha1 is higher than for Cha2 (0.13 vs. 0.07 mm/year, respectively). The Cha1 $\delta^{18}\text{O}$ record covers the period from 11.6 to -0.05 ka BP with two relatively short hiatuses (4.52–4.82 ka BP; 9.62–9.9 ka BP), whereas the Cha2 $\delta^{18}\text{O}$ record covers the period from 9.66 to -0.06 ka BP with a short hiatus from 0.21 to 0.39 ka BP and a relatively long hiatus from 1.15 to 1.76 ka BP. The average age model uncertainties of U-Th ages account for 33 and 41 years for Cha1 and Cha2, respectively. The mean resolution for the $\delta^{18}\text{O}$ records are 7 and 12 years for Cha1 and Cha2, respectively.

Monitoring in the cave area, reported by Wassenburg et al. (2016), showed that rainfall amount is well correlated to precipitation $\delta^{18}\text{O}$ ($r < -0.74$) and the winter NAO index ($r = -0.66$). Additionally, the stable isotope values of drip water samples from Grotte de Piste are consistent with the stable isotope values of the original rainfall (Text S1 and Figure S5). Therefore, we interpret the Cha1 and Cha2 records as proxy records of effective rainfall variability during the Holocene, whereby low $\delta^{18}\text{O}$ values reflect humid conditions and vice versa.

The comparison of the Cha1 and Cha2 records shows a high degree of replication (Figures 2a and 2b) when taking into account the different temporal resolutions, age uncertainties, and growth rate variations, which cannot be resolved by the age models. The average $\delta^{18}\text{O}$ value is -5.5‰ in both records. However, the $\delta^{18}\text{O}$ values range from -6.4‰ to -4.4‰ in the Cha1 record, and from -6.8‰ to -4.1‰ in the Cha2 record. Hence, the Cha1 record has a smaller $\delta^{18}\text{O}$ variability compared to the Cha2 record. This might be related to a longer water residence time, which results in a smoothing of the $\delta^{18}\text{O}$ precipitation signal (Mischel et al., 2015).

The Chaara cave record, described by a composite of the Cha1 and Cha2 $\delta^{18}\text{O}$ records (Figure 2c), shows $\delta^{18}\text{O}$ maxima of humid conditions in the Western Mediterranean that are synchronous with the GP2 speleothem record (Figure 2d), suggesting common forcing mechanisms. The comparison also reveals a few inconsistencies, which might be related to drip-site-specific conditions during the corresponding periods (Lachniet, 2009; Deininger et al., 2012), growth rate changes between dated intervals (Fohlmeister, 2012), and/or growth-rate-induced isotope fractionation (Fohlmeister et al., 2018). Another difference is the different amplitude of some positive and negative $\delta^{18}\text{O}$ peaks, which are synchronous in the three records when taking into account the age uncertainties and different resolutions. Hence, a representative rainfall index of the Western Mediterranean is constructed using the first axis of the PCA (PC1) between the Chaara composite and Grotte de Piste record. The PC1 accounts for 79% of their common variability (Table S3 and Figure 2e).

3.2. Western Mediterranean Climate and Linkage to the NAO During the Holocene

Maxima in humid conditions identified in each speleothem record are numbered in each time series in Figure 2. The rainfall index values show substantial multidecadal and centennial alternations of humid

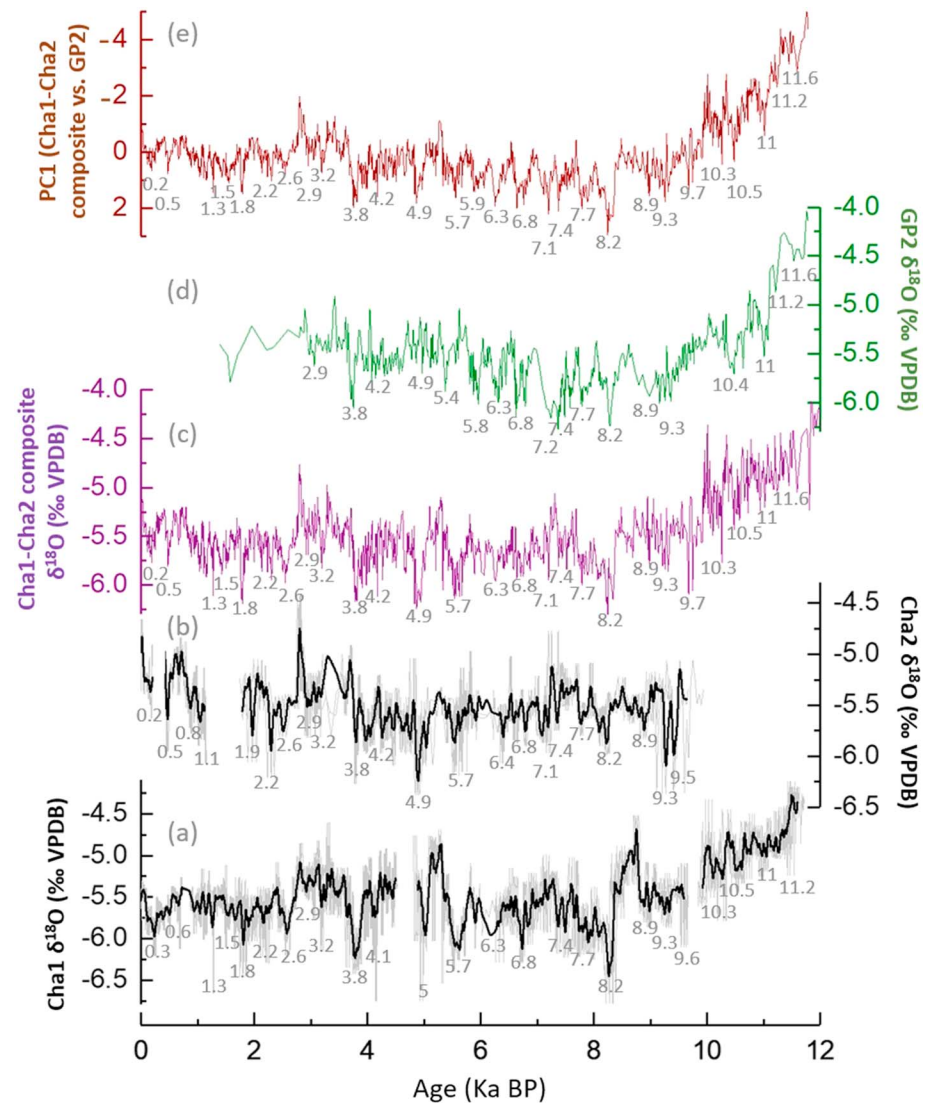


Figure 2. Comparison of proxy records from caves in Northern Morocco. (a, b) Cha1 and Cha2 speleothem $\delta^{18}\text{O}$ records from Chaara cave. The bold black curves show the 50-year moving average of each time series. The gray curves indicate the original data set, including the average, minus and plus age models. (c) Composite record of (a) and (b) constructed using intra-site correlation age modelling (Fohlmeister, 2012). (d) GP2 speleothem $\delta^{18}\text{O}$ record from Grotte de Piste. (e) Rainfall index constructed from the PC1 between (c) and (d). The gray numbers indicate the timing of peaks of humid conditions in the Western Mediterranean in kiloannum before present. VPDB = Vienna Pee Dee belemnite.

and dry conditions reflecting NAO-like precipitation patterns in the Western Mediterranean during the Holocene. Indeed, the comparison of the Western Mediterranean winter rain maxima and the NAO reconstructions (Ortega et al., 2015; Trouet et al., 2009) showed that negative NAO phases correspond to winter rain maxima in Moroccan speleothem records over the last millennium (Ait Brahim et al., 2018). This is also consistent with present-day climate patterns in the Western Mediterranean, where periods of increased winter rainfall are generally linked to negative modes of the NAO (Born et al., 2010; Hurrell et al., 2003; Knippertz et al., 2003; López-Moreno et al., 2011). Furthermore, the comparison with solar irradiance (Steinhilber et al., 2009, 2012) reveals that solar minima periods around 0.5, 2.2, 4.9, 5.7, 6.3, 8.2, and 8.9 ka BP seem to coincide within age error with $\delta^{18}\text{O}$ minima in the Western Mediterranean (Figure S6). This is consistent with present-day negative NAO patterns during periods of low solar activity (Matthes, 2011; Thiéblemont et al., 2015). The REDFIT spectral analysis reveals 200-year (Figure S7) periodicities in the speleothem records, similar to the Vries-Suess solar cycle (Suess, 1980), consistent with

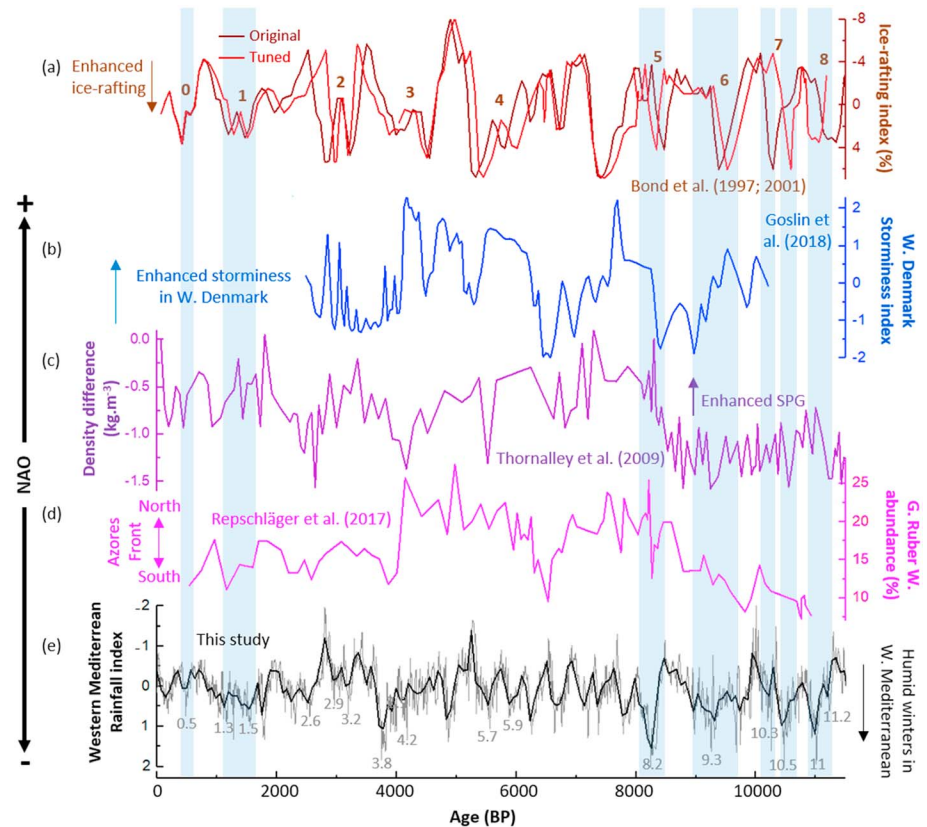


Figure 3. Comparison of the record of past rainfall variability in the Western Mediterranean derived from Moroccan speleothem $\delta^{18}\text{O}$ records with reconstructions of North Atlantic ocean and atmospheric modes. (a) North Atlantic ice-rafting records showing the tuned and the original record (Bond et al., 1997, 2001). The numbers indicate the timing of the eight Bond events. (b) Storminess index based on wind-blown coastal sand in the Western Denmark (Goslin et al., 2018 Corrigendum). (c) North Atlantic current activity, expressed by the activity of the subpolar gyre (SPG) based on the water-column density-difference (Thornalley et al., 2009). (d) Position of the AF and the extent of the subtropical gyre, based on the abundance of the planktonic foraminifera *Globigerinoides ruber* (*G. ruber* w.) in a sediment core in the vicinity of the Azores (Repschläger et al., 2017). (e) Detrended rainfall index of the Western Mediterranean, derived from speleothem $\delta^{18}\text{O}$ records (Cha1, Cha2, and GP2) from Northern Morocco. The black curve indicates the 70-year smoothing. The gray numbers indicate the timing of peaks of humid conditions in the Western Mediterranean (ka BP) within the periods of the Bond events. The blue shadings indicate the periods of overall humid conditions in the Western Mediterranean, which coincide within the age uncertainties with enhanced ice-rafting in the North Atlantic.

speleothem records of the last millennium from Morocco (Ait Brahim et al., 2017, 2018) and a lake record from the same region (Zielhofer et al., 2017).

3.3. North Atlantic Ocean and Atmospheric Dynamics During the IRD Events

In order to provide a detailed overview of the linkage between the Western Mediterranean rainfall and the ice-rafting on a centennial to millennial timescale, we compare our data with paleo-oceanographic and atmospheric reconstructions of the North Atlantic region. These include a record of the position of the AF and the extent of the subtropical gyre (STG; Repschläger et al., 2017; Figure 3d), a record of the activity of the subpolar gyre (SPG; Thornalley et al., 2009; Figure 3c) and a recent reconstruction of storminess from Western Denmark reflecting periods of enhanced northerly shifts of the westerly winds belt (akin to positive NAO; Figure 3b; Goslin et al., 2018).

On centennial to millennial timescales, the humid conditions during the Early Holocene (11.5 to 8 ka BP) seem to be more pronounced and prolonged with peaks around 8.2, 9.3, 10.3, 10.5, 11, and 11.2 ka BP (Figure 3e). Interestingly, the timing of these peaks recalls the well-known abrupt ice-rafting episodes in the North Atlantic high latitudes (Bond events 8, 7, 6, and 5; Figure 3a; Bond et al., 1997, 2001). The comparison of our rainfall index with the tuned IRD record shows a high positive correlation during this

period ($r = 0.6$; Figure S3). In contrast to Zielhofer et al. (2019) who suggest that dry winters prevailed in the Western Mediterranean in response to the Bond events during the Early Holocene, we propose southerly shifts of the westerly winds belt during these events resembling negative NAO-like conditions. Our data are confirmed by the SPG strength and the AF position reconstructions, which show that the period from 11.5 to 8 ka is characterized by a weak SPG, and hence an enhanced STG and southerly positioned AF, suggestive of a mean negative NAO-like state.

Interestingly, the glacial freshwater discharge event around 8.2 ka BP can be clearly identified in the Western Mediterranean. This event marks a transition toward enhanced SPG, weaker STG and a northerly shift of the AF. These conditions mark a transition from predominantly negative NAO-like conditions during the Early Holocene toward more positive NAO-like conditions during the mid-Holocene, consistent with $\delta^{18}\text{O}$ gradients in European speleothems which reveal a switch from negative to positive NAO at about 8 ka BP (Deininger et al., 2016). Furthermore, the timing of this transition is close to a major reorganization of the NAO around 8.5 ka BP as a response to the presence of the Laurentide Ice Sheet and meltwater fluxes into the North Atlantic (Wassenburg et al., 2016). Subsequent modern positive NAO-like conditions were associated with northeasterly and southwesterly shifts of the IL and AH, respectively.

During the mid-Holocene (8 to 4 ka BP), our record shows substantial alternations of wet and dry periods on centennial timescales. Contrary to the Early Holocene, enhanced ice-rafting periods (around 7.5 ka BP and Bond events 4 and 3) do not coincide with prolonged humid conditions in the Western Mediterranean. Moreover, the correlation between the Western Mediterranean rainfall index and the tuned IRD record is not significant during this period. However, these events are characterized by relatively more enhanced SPG, northern shifts of the AF and the westerly winds belt, akin to predominantly positive NAO, during all the ice-rafting events of the mid-Holocene.

After 4 ka, a shift toward more humid conditions is observed in the Western Mediterranean with a peak centered on 3.8 ka BP. This shift coincides with an abrupt southern shift of the AF and an overall reduced SPG, marking a temporary passage toward negative NAO-like conditions. However, wet conditions are not clearly observed in the Western Mediterranean during the subsequent ice-rafting event around 2.8 ka (Bond event 2). Instead, the 2.8 ka BP event shows similar patterns of the SPG and the AF as the 4.2- and 5.8-ka BP events, which suggest northern shifts of the westerly winds belt as also evidenced by the enhanced storminess in Western Denmark.

During the last 2 ka, wet conditions are observed in the Western Mediterranean with peaks around 1.5, 1.3, and 0.5 BP, coincident with the timing of ice-rafting events (Bond events 1 and the Little Ice Age “LIA”) suggesting a predominance of negative NAO-like conditions. Indeed, the 1.5-ka event coincides with relatively reduced SPG and south shift of the AF. The LIA, shortest Bond event, is also characterized by low SPG. While the AF record does not extend until the end of the LIA, the southern shift of the westerly winds belt during the LIA is proposed by the NAO reconstructions during the last millennium (e.g., Trouet et al., 2009). A high positive correlation is also observed between our rainfall index and the IRD record during the last two millennia ($r = 0.6$).

3.4. Proposed Mechanisms and Potential Linkages Between the NAO and the Bond Events

Based on the above, we show that there is no persistency of negative or positive NAO-like phases during all the periods of enhanced North Atlantic ice-rafting (Bond events). The occurrence of the ice-rafting events during periods of prolonged positive and negative NAO-like conditions, suggests that the role of the westerly winds belt in triggering the abrupt cooling events of the Holocene might have been overestimated, at least during some of the Bond events. However, different feedback mechanisms may have been involved, possibly linked to the mean state of the NAO during the Holocene on millennial timescales. Depending on the mean state of the NAO on millennial timescales, the centennial variability of NAO-like patterns may have been associated with either extreme negative or positive NAO-like conditions. For example, a centennial-scale negative (positive) NAO-like phase during a period of predominant mean negative (positive) state on millennial timescales might result in extreme negative (positive) NAO-like conditions. As such, the prolonged periods of north and south shifts of the westerly winds belt might have both resulted in triggering or amplifying the ice-rafting events. These mechanisms are associated with changes in the strength of the STG (Morley et al., 2011) and possibly influenced by solar forcing (Moffa-Sanchez et al., 2014).

Indeed, the Holocene ice-rafting events with predominant negative NAO-like conditions (LIA and Bond events 1, 5, 6, 7, and 8) might be linked to a reduction in North Atlantic Deep Water (NADW) formation. Therefore, the slowdown of the AMOC might have been triggered or amplified by reduced wind stress resulting from southern shifts of the westerly winds belt (Deininger et al., 2016; Mangini et al., 2007; Moffa-Sánchez & Hall, 2017). The AMOC slowdown gives rise to a cooling and a subsequent expansion of sea ice in the North Atlantic high latitudes (Deininger et al., 2016). This is in line with modeling results, which suggest a southward expansion of sea ice as a positive feedback mechanism for a reduced AMOC during periods of reduced wind stress on the North Atlantic (Sanchez-Gomez et al., 2016; Yang et al., 2016).

However, we propose that enhanced ice-rafting might have taken place in the northern North Atlantic during periods with predominant positive NAO-like patterns as well (Bond events 2, 3, and 4 and around 7.5 ka BP). Indeed, north shifts of the westerly winds belt have also been proposed as a potential amplifier of the pluricentennial ice-rafting events (Goslin et al., 2018; Klus et al., 2018). Strong northerly winds were suggested as a potential trigger of ice drifting by strengthening the polar vortex and cooling at polar and sup-polar latitudes (Bond et al., 2001). Accordingly, the AMOC slowdown is possibly a feedback mechanism of the strong SPG.

4. Conclusions

North Morocco is one of the most sensitive regions to the NAO, and its associated westerly winds circulation in the Western Mediterranean. High-resolution speleothem records from this region, presented in this study, are interpreted as proxy records of effective rainfall resulting from southern shifts of the westerly winds belt related to negative NAO-like conditions during the Holocene.

NAO-like conditions evolved during the Holocene as a response to different forcing mechanisms, such as changes in the insolation and the meltwater input into the North Atlantic Ocean. We propose that predominantly negative NAO-like conditions occurred during the ice-rafting events of the Early Holocene and the Late Holocene, whereas positive NAO-like patterns might have probably prevailed during the ice-rafting periods of the mid-Holocene. Therefore, in contrast to previous assumptions about the linkage between the NAO and ice-rafting in the North Atlantic high latitudes, we conclude that there is no persistency of either positive or negative NAO-like conditions during all the North Atlantic ice-rafting events of the Holocene. Clearly, different mechanisms can trigger or amplify ice-rafting. Prolonged southward shifts of the westerly winds belt might have played a role in causing the slowdown of the AMOC and the enhanced ice-rafting due to a reduced wind stress on the North Atlantic Ocean during the Early and the Late Holocene, whereas northward shifts of westerly winds belt were proposed as a potential amplifier of cooling and enhanced ice-rafting by strengthening the polar vortex during the mid-Holocene.

Data Availability Statement

After acceptance of the manuscript, the data produced here will be made available in the public paleoclimate databases of NOAA and SISAL.

References

- Ait Brahim, Y., Cheng, H., Sifeddine, A., Wassenburg, J., Cruz, F. W., Khodri, M., et al. (2017). Speleothem records decadal to multidecadal hydroclimate variations in southwestern Morocco during the last millennium. *Earth and Planetary Science Letters*, 476, 1–10. <https://doi.org/10.1016/j.epsl.2017.07.045>
- Ait Brahim, Y., Wassenburg, J. A., Cruz, F. W., Sifeddine, A., Scholz, D., Bouchaou, L., et al. (2018). Multi-decadal to centennial hydroclimate variability and linkage to solar forcing in the Western Mediterranean during the last 1000 years. *Scientific Reports*, 8, 17446. <https://doi.org/10.1038/s41598-018-35498-x>
- Baker, A., Hellstrom, J. C., Kelly, B. F. J., Mariethoz, G., & Trouet, V. (2015). A composite annual-resolution stalagmite record of North Atlantic climate over the last three millennia. *Scientific Reports*, 5(1), 10307. <https://doi.org/10.1038/srep10307>
- Benito, G., Macklin, M. G., Zielhofer, C., Jones, A. F., & Machado, M. J. (2014). Holocene flooding and climate change in the Mediterranean. *Catena*, 130, 13–33.
- Bond, G., Kromer, B., Beer, J., Muscheler, R., Evans, M. N., Showers, W., et al. (2001). Persistent solar influence on North Atlantic climate during the Holocene. *Science*, 294(5549), 2130–2136. <https://doi.org/10.1126/science.1065680>
- Bond, G., Showers, W., Cheseby, M., Lotti, R., Almasi, P., deMenocal, P., et al. (1997). A pervasive millennial-scale cycle in North Atlantic Holocene and glacial climates. *Science*, 278(5341), 1257–1266. <https://doi.org/10.1126/science.278.5341.1257>
- Born, K., Fink, A. H., & Knippertz, P. (2010). Meteorological processes influencing the weather and climate of Morocco. In P. Speth, M. Christoph, & B. Diekkrüger (Eds.), *Impacts of Global Change on the Hydrological Cycle in West and Northwest Africa* (pp. 150–163). Berlin Heidelberg: Springer-Verlag.

Acknowledgments

The authors thank the Editor and the four anonymous reviewers for their constructive comments. This work was sponsored thanks to the National Natural Science Foundation of China (NSFC 41888101 and NSFC 41731174) to H. C., the Postdoctoral Science Foundation of China (2018M640971) to Y. A., Fundação de Amparo a Pesquisa do Estado de São Paulo, Brazil (FAPESP Grant 2017/50085-3) and the CLIMACTE Tripartite Cooperative Project (IRD-France/CNPq-Brazil/APGMV-Africa 457400/2012-9) grant to F. W. C. and A. S., the German Research Foundation (DFG) Grants WA3532/1-1 to J. A. W. and DE 2398/3-1 to M. D., and the U.S. National Science Foundation (NSF 1702816) to R. L. E. and H. C. We would like to thank Alyne Barros for her assistance with the stable isotope analyses and Li Hanying for her help with the statistical analyses. We are also grateful to Augusto Auler, Jean-Loup Guyot, El Hassane Beraaouz, and the Associations of Speleologists in Agadir (ASS and ASA) for their help during fieldwork. The authors declare no conflict of interest.

- Darby, D. A., Ortiz, J. D., Grosh, C. E., & Lund, S. P. (2012). 1,500 cycle in the Arctic Oscillation identified in Holocene Arctic sea-ice drift. *Nature Geoscience*, 5(12), 897–900. <https://doi.org/10.1038/ngeo1629>
- Deininger, D., Werner, M., & McDermott, F. (2016). North Atlantic Oscillation controls on oxygen and hydrogen isotope gradients in winter precipitation across Europe: Implications for palaeoclimate studies. *Climate of the Past*, 12(11), 2127–2143. <https://doi.org/10.5194/cp-12-2127-2016>
- Deininger, M., Fohlmeister, J., Scholz, D., & Mangini, A. (2012). Isotope disequilibrium effects: the influence of evaporation and ventilation effects on the carbon and oxygen isotope composition of speleothems – a model approach. *Geochimica et Cosmochimica Acta*, 96, 57–79. <https://doi.org/10.1016/j.gca.2012.08.013>
- Deininger, M., McDermott, F., Mudelsee, M., Werner, M., Frank, N., & Mangini, A. (2017). Coherency of late Holocene European speleothem $\delta^{18}\text{O}$ records linked to North Atlantic Ocean circulation. *Climate Dynamics*, 49(1-2), 595–618. <https://doi.org/10.1007/s00382-016-3360-8>
- Edwards, R. L., Chen, J. H., & Wasserburg, G. J. (1987). ^{238}U - ^{234}U - ^{230}Th - ^{232}Th systematics and the precise measurement of time over the past 500,000 y. *Earth and Planetary Science Letters*, 81(2-3), 175–192. [https://doi.org/10.1016/0012-821X\(87\)90154-3](https://doi.org/10.1016/0012-821X(87)90154-3)
- Fletcher, W. J., Debret, M., & Goni, M. F. S. (2013). Mid-Holocene emergence of a low-frequency millennial oscillation in western Mediterranean climate: Implications for past dynamics of the North Atlantic atmospheric westerlies. *Holocene*, 23(2), 153–166. <https://doi.org/10.1177/0959683612460783>
- Fohlmeister, J. (2012). A statistical approach to construct composite climate records of dated archives. *Quaternary Geochronology*, 14, 48–56. <https://doi.org/10.1016/j.quageo.2012.06.007>
- Fohlmeister, J., Arps, J., Spötl, C., Schröder-Ritzrau, A., Plessen, B., Günter, C., et al. (2018). Carbon and oxygen isotope fractionation in the water-calcite-aragonite system. *Geochimica et Cosmochimica Acta*, 235, 127–139. <https://doi.org/10.1016/j.gca.2018.05.022>
- Goslin, J., Fruergaard, M., Sander, L., Galka, M., Menviel, L., Monkenbush, J., et al. (2018). Holocene centennial to millennial shifts in North-Atlantic storminess and ocean dynamics. *Scientific Reports*, 8(1), 12778, Corrigendum. <https://doi.org/10.1038/s41598-018-29949-8>
- Hammer, Ø., Harper, D. A. T., & Ryan, P. D. (2001). PAST: paleontological statistics software package for education and data analysis. *Palaeontologia Electronica*, 4, 9.
- Hurrell, J. W. (1995). Decadal trends in the North-Atlantic Oscillation—Regional temperatures and precipitation. *Science*, 269(5224), 676–679. <https://doi.org/10.1126/science.269.5224.676>
- Hurrell, J. W., Kushnir, Y., Ottersen, G., & Visbeck, M. (2003). An overview of the North Atlantic oscillation. In J. W. Hurrell, Y. Kushnir, G. Ottersen, & M. Visbeck (Eds.), *The North Atlantic Oscillation: Climatic Significance and Environmental Impact, Geophysical Monograph Series*, (Vol. 5, pp. 1–35). Washington: American Geophysical Union.
- Jones, P. D., Jónsson, T., & Wheeler, D. (1997). Extension to the North Atlantic Oscillation using early instrumental pressure observations from Gibraltar and South-West Iceland. *International Journal of Climatology*, 17(13), 1433–1450. [https://doi.org/10.1002/\(SICI\)1097-0088\(199711\)17:13<1433::AID-JOC203>3.0.CO;2-P](https://doi.org/10.1002/(SICI)1097-0088(199711)17:13<1433::AID-JOC203>3.0.CO;2-P)
- Kim, S.-T., Mucci, A., & Taylor, B. E. (2007). Phosphoric acid fractionation factors for calcite and aragonite between 25 and 75 degrees C: Revisited. *Chemical Geology*, 246(3-4), 135–146. <https://doi.org/10.1016/j.chemgeo.2007.08.005>
- Klus, A., Prange, M., Varma, V., Tremblay, L. B., & Schulz, M. (2018). Abrupt cold events in the North Atlantic in a transient Holocene simulation. *Climate of the Past*, 14(8), 1165–1178. <https://doi.org/10.5194/cp-14-1165-2018>
- Knippertz, P., Christoph, M., & Speth, P. (2003). Long-term precipitation variability in Morocco and the link to the large-scale circulation in recent and future climates. *Meteorology and Atmospheric Physics*, 83(1-2), 67–88. <https://doi.org/10.1007/s00703-002-0561-y>
- Lachniet, M. S. (2009). Climatic and environmental controls on speleothem oxygen-isotope values. *Quaternary Science Reviews*, 28(5-6), 412–432. <https://doi.org/10.1016/j.quascirev.2008.10.021>
- López-Moreno, J. I., Vicente-Serrano, S. M., Moran-Tejeda, E., Lorenzo-Lcrúz, J., Kenawy, A., & Beniston, M. (2011). Effects of the North Atlantic Oscillation (NAO) on combined temperature and precipitation winter modes in the Mediterranean mountains: Observed relationships and projections for the 21st Century. *Global and Planetary Change*, 77(1-2), 62–76. <https://doi.org/10.1016/j.gloplacha.2011.03.003>
- Mangini, A., Verdes, P., Spötl, C., Scholz, D., Vollweiler, N., & Kromer, B. (2007). Persistent influence of the North Atlantic hydrography on central European winter temperature during the last 9000 years. *Geophysical Research Letters*, 34, L02704. <https://doi.org/10.1029/2006gl028600>
- Matthes, K. (2011). Atmospheric science: solar cycle and climate predictions. *Nature Geoscience*, 4(11), 735–736. <https://doi.org/10.1038/ngeo1298>
- McDermott, F., Atkinson, T. C., Fairchild, I. J., Baldini, L. M., & Matthey, D. P. (2011). A first evaluation of the spatial gradients in $\delta^{18}\text{O}$ recorded by European Holocene speleothems. *Global and Planetary Change*, 79(3-4), 275–287. <https://doi.org/10.1016/j.gloplacha.2011.01.005>
- Mischel, S. A., Scholz, D., & Spötl, C. (2015). $\delta^{18}\text{O}$ values of cave drip water: A promising proxy for the reconstruction of the North Atlantic Oscillation? *Climate Dynamics*, 45(11-12), 3035–3050. <https://doi.org/10.1007/s00382-015-2521-5>
- Moffa-Sánchez, P., Born, A., Hall, I. R., Thornalley, D. J. R., & Barker, S. (2014). Solar forcing of North Atlantic surface temperature and salinity over the past millennium. *Nature Geoscience*, 7(4), 275–278. <https://doi.org/10.1038/ngeo2094>
- Moffa-Sánchez, P., & Hall, I. R. (2017). North Atlantic variability and its links to European climate over the last 3000 years. *Nature Communications*, 8(1), 1726. <https://doi.org/10.1038/s41467-017-01884-8>
- Morellón, M., Aranbarri, J., Moreno, A., González-Sampériz, P., & Valero-Garcés, B. L. (2018). Early Holocene humidity patterns in the Iberian Peninsula reconstructed from lake, pollen and speleothem records. *Quaternary Science Reviews*, 181, 1–18. <https://doi.org/10.1016/j.quascirev.2017.11.016>
- Morley, A., Schulz, M., Rosenthal, Y., Multiza, S., Paul, A., & Rühlemann, C. (2011). Solar modulation of North Atlantic central water formation at multidecadal timescales during the late Holocene. *Earth and Planetary Science Letters*, 308(1-2), 161–171. <https://doi.org/10.1016/j.epsl.2011.05.043>
- Olsen, J., Anderson, J. N., & Knudsen, M. F. (2012). Variability of the North Atlantic Oscillation over the past 5200 years. *Nature Geoscience*, 5(11), 808–812. <https://doi.org/10.1038/ngeo1589>
- Ortega, P., Lehner, F., Swingedouw, D., Masson-Delmotte, V., Raible, C. C., Casado, M., & Yiou, P. (2015). A model-tested North Atlantic Oscillation reconstruction for the past millennium. *Nature*, 523(7558), 71–74. <https://doi.org/10.1038/nature14518>
- Repschläger, J., Garbe-Schönberg, D., Weinelt, M., & Schneider, R. (2017). Holocene evolution of the North Atlantic subsurface transport. *Climate of the Past*, 13(4), 333–344. <https://doi.org/10.5194/cp-13-333-2017>

- Sabaoui, A., Obda, K., & Laouane, M. (2009). Potentialités géologiques du développement local du Moyen Atlas septentrional: structures, paysages et histoire géologique. *Geomaghreb*, 5, 9–39.
- Sanchez-Gomez, E., Cassou, C., Ruprich-Robert, Y., Fernandez, E., & Terray, L. (2016). Drift dynamics in a coupled model initialized for decadal forecasts. *Climate Dynamics*, 46(5–6), 1819–1840. <https://doi.org/10.1007/s00382-015-2678-y>
- Schneider, U., Becker, A., Finger, P., Meyer-Christoffer, A., Rudolf, B., Ziese, M. (2011). GPCP full data reanalysis version 6.0 at 1.0°: monthly land-surface precipitation from rain-gauges built on GTS-based and historic data. https://doi.org/10.5676/DWD_GPCC/FD_M_V6_100
- Scholz, D., & Hoffmann, D. L. (2011). StalAge—An algorithm designed for construction of speleothem age models. *Quaternary Geochronology*, 6(3–4), 369–382. <https://doi.org/10.1016/j.quageo.2011.02.002>
- Schulz, M., & Mudelsee, M. (2002). REDFIT: estimating red-noise spectra directly from unevenly spaced paleoclimatic time-series. *Computers and Geosciences*, 28(3), 421–426. [https://doi.org/10.1016/S0098-3004\(01\)00044-9](https://doi.org/10.1016/S0098-3004(01)00044-9)
- Sorrel, P., Debret, M., Billeaud, I., Jaccard, S. L., McManus, J. F., & Tessier, B. (2012). Persistent non-solar forcing of Holocene storm dynamics in coastal sedimentary archives. *Nature Geoscience*, 5(12), 892–896. <https://doi.org/10.1038/ngeo1619>
- Steinhilber, F., Abreu, J. A., Beer, J., Brunner, I., Christl, M., Fischer, H., et al. (2012). 9,400 years of cosmic radiation and solar activity from ice cores and tree rings. *Proceedings of the National Academy of Sciences*, 109(16), 5967–5971. <https://doi.org/10.1073/pnas.1118965109>
- Steinhilber, F., Beer, J., & Frohlich, C. (2009). Total solar irradiance during Holocene. *Geophysical Research Letters*, 36, L19704. <https://doi.org/10.1029/2009GL040142>
- Suess, H. E. (1980). The radiocarbon record in tree rings of the last 8000 years. *Radiocarbon*, 22(2), 200–209. <https://doi.org/10.1017/S0033822200009462>
- Taous, A., Tribak, A., Obda, K., Baena, E. R., Lopez, L., Enrique, J., & Miranda Bonilla, J. (2009). Karst et ressources en eau au Moyen Atlas nord-oriental. *Geomaghreb*, 5, 41–59.
- Thiéblemont, R., Matthes, K., Omrani, N. E., Kodera, K., & Hansen, F. (2015). Solar forcing synchronizes decadal North Atlantic climate variability. *Nature Communications*, 6(1), 8268. <https://doi.org/10.1038/ncomms9268>
- Thornalley, D. J. R., Elderfield, H., & McCave, I. N. (2009). Holocene oscillations in temperature and salinity of the surface subpolar North Atlantic. *Nature*, 457(7230), 711–714. <https://doi.org/10.1038/nature07717>
- Trouet, V., Esper, J., Graham, N. E., Baker, A., Scourse, J. D., & Frank, D. C. (2009). Persistent positive North Atlantic Oscillation mode dominated the medieval climate anomaly. *Science*, 324(5923), 78–80. <https://doi.org/10.1126/science.1166349>
- Visbeck, M. H., Hurrell, J. W., Polvani, L., & Cullen, H. M. (2001). The North Atlantic Oscillation: Past, present, and future. *Proceedings of the National Academy of Sciences of the United States of America*, 98(23), 12,876–12,877. <https://doi.org/10.1073/pnas.231391598>
- Walczak, I. W., Baldini, J. U. L., Baldini, L. M., McDermott, F., Marsden, S., Standish, C. D., et al. (2015). Reconstructing high-resolution climate using CT scanning of unsectioned stalagmites: A case study identifying the mid-Holocene onset of the Mediterranean climate in southern Iberia. *Quaternary Science Reviews*, 127, 117–128. <https://doi.org/10.1016/j.quascirev.2015.06.013>
- Wang, Y. H., Gudrun, M., Stern, H., Tian, X., & Yu, Y. (2012). Decadal variability of the NAO: Introducing an augmented NAO index. *Geophysical Research Letters*, 39, L21702. <https://doi.org/10.1029/2012gl053413>
- Wanner, H., Bronnimann, S., Casty, C., Gyalistras, D., Luterbacher, J., Schmutz, C., et al. (2001). North Atlantic Oscillation—Concepts and studies. *Surveys in Geophysics*, 22(4), 321–381. <https://doi.org/10.1023/A:1014217317898>
- Wassenburg, J. A., Dietrich, S., Fietzke, J., Fohlmeister, J., Jochum, K. P., Scholz, D., et al. (2016). Reorganization of the North Atlantic Oscillation during Early Holocene deglaciation. *Nature Geoscience*, 9(8), 602–605. <https://doi.org/10.1038/ngeo2767>
- Wassenburg, J. A., Immenhauser, A., Richter, D. K., Jochum, K. P., Fietzke, J., Deininger, M., et al. (2012). Climate and cave control on Pleistocene/Holocene calcite-to-aragonite transitions in speleothems from Morocco: elemental and isotopic evidence. *Geochimica et Cosmochimica Acta*, 92, 23–47. <https://doi.org/10.1016/j.gca.2012.06.002>
- Yang, H., Wang, K., Dai, H., Wang, Y., & Li, Q. (2016). Wind effect on the Atlantic meridional overturning circulation via sea ice and vertical diffusion. *Climate Dynamics*, 46(11–12), 3387–3403. <https://doi.org/10.1007/s00382-015-2774-z>
- Zielhofer, C., Fletcher, W. J., Mischke, S., De Batist, M., Campbell, J. F. E., Joanin, S., et al. (2017). Atlantic forcing of Western Mediterranean winter rain minima during the last 12,000 years. *Quaternary Science Reviews*, 157, 29–51. <https://doi.org/10.1016/j.quascirev.2016.11.037>
- Zielhofer, C., Köhler, A., Mischke, S., Benkaddour, A., Mikdad, A., & Fletcher, W. J. (2019). Western Mediterranean hydro-climatic consequences of Holocene ice-rafted debris (Bond) events. *Climate of the Past*, 15(2), 463–475. <https://doi.org/10.5194/cp-15-463-2019>